CrystEngComm

Accepted Manuscript

This article can be cited before page numbers have been issued, to do this please use: D. Chen, L. Lin, T. Sheng, Y. Wen, S. Hu, R. Fu, C. Zhuo, H. Li and X. Wu, *CrystEngComm*, 2017, DOI: 10.1039/C7CE00361G.

ROYAL SOCIETY OF CHEMISTRY

rsc.li/crystengcomm

View Article Online
DOI: 10.1039/C7CE00361G

CrystEngComm

ARTICLE

Syntheses, structures and luminescence properties of five coordination polymers based on designed 2,7-bis(4-benzoic acid)-N-(4-benzoic acid) carbazole

Received 00th January 20xx,
Accepted 00th January 20xx

DOI: 10.1039/x0xx00000x

www.rsc.org/

Dong-Hui Chen[ab], Ling Lin[ab], Tian-Lu Sheng[a], Yue-Hong Wen[a], Sheng-Min Hu[a], Rui-Biao Fu[a], Chao Zhuo[ab], Hao-Ran Li[ab] and Xin-Tao Wu*[a]

Herein we report five porous luminescent coordination polymers (CPs), $[Zn_3(\mathbf{L_{27}})_2(DMA)_6(H_2O)_4]_n$ (**TCZ-001**), $[Zn_3(\mathbf{L_{27}})_2(DMA)_6(CH_3CH_2OH)_2]_n$ (**TCZ-002**), $[Zn_3(\mathbf{L_{27}})_2(DMA)_6(CH_3OH)]_n$ (**TCZ-003**), $[Cd_3(\mathbf{L_{27}})_2(DMA)_6(H_2O)_2]_n$ (**TCZ-004**), $[Cd_9(\mathbf{L_{27}})_6DMA_{13}(4,4'\text{-BPY})_2(OH)_2(H_2O)_{13.5}]_n$ (**TCZ-005**) [$\mathbf{H_3L_{27}}$ = 2,7-bis(4-benzoic acid)-N-(4-benzoic acid) carbazole, DMA = N,N-dimethylacetamide, 4,4'-BPY = 4,4'-bipyridine, TCZ = "T"-shape carbazole-based polymers, $\mathbf{L_{27}}$ = fully deprotonated $\mathbf{H_3L_{27}}^{3-}$ ligand]. All of the five CPs were assembled from a novel luminescent carbazole-based ligand. X-ray crystallography showed that **TCZ-001** is a 3-connected one-dimensional (1D) chain structure with a $\{4^2.6\}$ topology. **TCZ-002** possesses a 3,6-connected three-dimensional (3D) framework with a point symbol of $\{4^2.6\}_2\{4^4.6^2.8^7.10^2\}$. **TCZ-003** displays a 3,6-connected two-dimensional 2D network with a Schläfli symbol of $\{4^{11}.6^4\}.\{4^3\}_2$, which is a new topology. **TCZ-004** features a 3,6-connected 2D net with a $\{4^3\}_2.\{4^6.6^6.8^3\}$ topology. In **TCZ-005**, the structure can be classified into two groups: One of the two groups is a 3-connected 1D chain structure with a $\{4^2.6\}$ topology, similar to **TCZ-001**; The other one possesses a 3,3,3,4-connected network with a Schläfli symbol of $\{4^2.6^3.8\}\{4^2.6\}_3$. The structure of **TCZ-005** could be described as a SP 1-periodic net (4,4)(0,2) in the 1D_2D.ttd database. **TCZ-001**, **TCZ-003** and **TCZ-004** show a remarkable response to Ni^{2+} concentration in DMA, H_2O or EtOH. Part of Zn^{2+} ions were replaced by Ni^{2+} ions and the rate of the transmetalation depended on the concentration of Ni^{2+} ions. And changing part of the metal node would transform the colour of emmitting light. Additionally, the colour of the luminescent display a linear correlation with the Ni^{2+} concentration range from 0.005 to 0.35M (mol/L). Besides selective sensing of Ni^{2+}, **TCZ-004** can also be utilized to detect Eu^{3+} in DMA solution. Thus, several potential sensory probe materials for Ni^{2+} and Eu^{3+} detection in DMA solution have been obtained.

Introduction

Coordination polymers (CPs) or metal-organic complexes (MOCs), assembled from organic linkers and metal nodes, have been explored for potential application in fluorescence sensors,[1-4] separation,[5] gas sorption[6,7] and catalysis.[8] The flexibility of organic linkers and metal nodes provides the opportunity for engineering the optical properties[2,4] and structure of the CPs.[9] Recently a recent surging in luminescent CPs utilized to detect metal ions, volatile organic compounds and anions,[10-18] especially in detecting heavy and lanthanide metal ions, such as Co^{2+}, Cu^{2+}, Mn^{2+}, Ag^{+}, Zn^{2+}, Cd^{2+}, Hg^{2+}, Cr^{6+}, Fe^{3+}, Eu^{3+} and Tb^{3+}.[19-29] But selectively detecting Ni^{2+} ion remains rare. Moreover, sensing Ni^{2+} ions concentration according to colour of the emitting light is much more infrequent. Undoubtedly, luminescence-based detection of Ni^{2+} ions concentration is much simpler than the traditional method by the dimethylgyoxmine spectrophotometry, which need professional technician and instrument.[30] And another method that figuring out the ions concentration is basing on the intensity of the emission spectra of probe material in various concentrations of ions. But this method requires confirming the standards before measuring.[31,32] Therefore, a more convenient and rapid method need to be created and used in detecting Ni^{2+} concentration. Meanwhile, sensing Eu^{3+} concentration in DMA solution rapidly based on the colour of emitting light is also unusual. Herein, a family of new CPs was designed specifically to address this problem and the solution to this can be explored with a focus on the luminescent property of the ligand.

Carbazole, a star aromatic compound, is commonly found in fluorescence molecules and used to synthesize stable optoelectronic materials. Reason for the wide application of carbazole-based polymers is owing to their excellent thermal and photochemical stability, outstanding hole transporting ability and large conjugated π system.[33,34] Carbazole could be

[a.] State Key Laboratory of Structure Chemistry, Fujian Institute of Research on the Structure of Matter, Chinese Academy of Sciences, Fuzhou 350002, Fujian, PR China.
E-mail: wxt@fjirsm.ac.cn
[b.] University of the Chinese Academy of Sciences, Beijing, 100049, China.

Electronic Supplementary Information (ESI) available: Selected bond lengths and angles, PXRD curve, TGA curve, IR spectra, CCDC-1527984 for TCZ-001, CCDC-1527985 for TCZ-002, CCDC-1527986 for TCZ-003, CCDC-1527987 for TCZ-004, CCDC-1527988 for TCZ-005. For ESI and crystallographic data in CIF or other electronic format see DOI: 10.1039/x0xx00000x.

View Article Online DOI: 10.1039/C7CE00361G

functionalized at (3,6-), (2,7-) , or N positions. 2, 7-carbazole-based polymers have lower band gap and better fluorescent property, and functionalized at N positions is beneficial to self-assembling of the porous structure.[35-38] Considering these properties of carbazole-based polymers, 2,7-bis(4-benzoic acid)-N-(4-benzoic acid) carbazole (**H_3L_{27}**) was designed and synthesized based on the fact that the appended benzoic acid moieties will significantly increase the size of the ligand.[39-47]

Due to the nature of **H_3L_{27}**, a conjugated tricarboxylic acid ligand, its reaction with Zn^{II} and Cd^{II} salts was predicted to form 1D to 3D structure coordination polymer based on different metal clusters nodes. Herein, we present five CPs, $[Zn_3(\mathbf{L_{27}})_2(DMA)_6(H_2O)_4]_n$ (**TCZ-001**), $[Zn_3(\mathbf{L_{27}})_2(DMA)_6(EtOH)_2]_n$ (**TCZ-002**), $[Zn_3(\mathbf{L_{27}})_2(DMA)_6(CH_3OH)]_n$ (**TCZ-003**), $[Cd_3(\mathbf{L_{27}})_2(DMA)_6(H_2O)_2]_n$ (**TCZ-004**), $[Cd_9(\mathbf{L_{27}})_6DMA_{13}(4,4'\text{-BPY})_2(OH)_2(H_2O)_{13.5}]_n$ (**TCZ-005**) (DMA = N,N-dimethylacetamide, 4,4'-BPY = 4,4'-bipyridine, TCZ= "T"-shape carbazole-based polymers).

Experimental section

Materials and Methods

4,4'-dibromobiphenyl, potassium tert-butoxide, ethyl 4-fluorobenzoate, potassium carbonate, tetrakis(triphenylphosphine)palladium(0), $Zn(NO_3)_2{\cdot}6H_2O$, $Cd(NO_3)_2{\cdot}6H_2O$ and solvents were purchased commercially and used directly. Elemental analyses (C, H and N) were performed with an Elementar Vario EL-Cube Element Analyzer. Powder X-ray diffraction (PXRD) data were collected on a Rigaku MiniFlex 600 diffractometer using Cu Kα radiation (λ = 0.154 nm). Infrared spectra were recorded with KBr pellets in the range 4000-400cm^{-1} on a Perkin-Elmer Spectrum One FT-IR spectrometer. Thermogravimetric analysis (TGA) experiments were carried out on a NETZSCH STA 449C Jupiter thermogravimetric analyzer in flowing nitrogen with the sample heated in an Al_2O_3 crucible from room temperature to 1000 °C at a heating rate of 10 K min^{-1}. Metal elemental analyses (for Zn, Ni and Eu) were performed with a HORIBA Jobin Yvon Ultima2 Inductively Coupled Plasma OES spectrometer (ICP).

4,4'-Dibromo-2-nitrobiphenyl(1): Compound **1** was synthesized followed the reported procedure.[42] 4,4'-dibromobiphenyl (20.0 g, 64.1 mmol) was dissolved in glacial acetic acid (300 mL), and the mixture was stirred and heated to 110 °C. When 4,4'-Dibromobiphenyl was dissolved totally, fuming concentrated nitric acid (95%, 80 mL) was added slowly to the solution. Then, heating the mixture at 110 °C until the precipitate formed after adding fuming concentrated nitric acid was redissolved. The solution was cooled to room temperature and the resulting solid was collected by filtration. After recrystallisation from EtOH, 4,4'-Dibromo-2-nitrobiphenyl was obtained as a yellow solid (20.8 g, 91% yield). ^{1}H NMR (400 MHz, $CDCl_3$): δ (ppm) = 8.05 (d, *J* = 1.96 Hz, 1 H), 7.78 (dd, *J* = 6.24, 2.00 Hz, 1 H), 7.78 (d, *J* = 8.44 Hz, 2 H), 7.31 (d, *J* = 8.28 Hz, 1H), 7.18 (d, *J* = 8.40 Hz, 2 H). ^{13}C NMR (400 MHz, $CDCl_3$): δ (ppm) = 149.23, 135.60, 135.30, 134.14, 133.04,

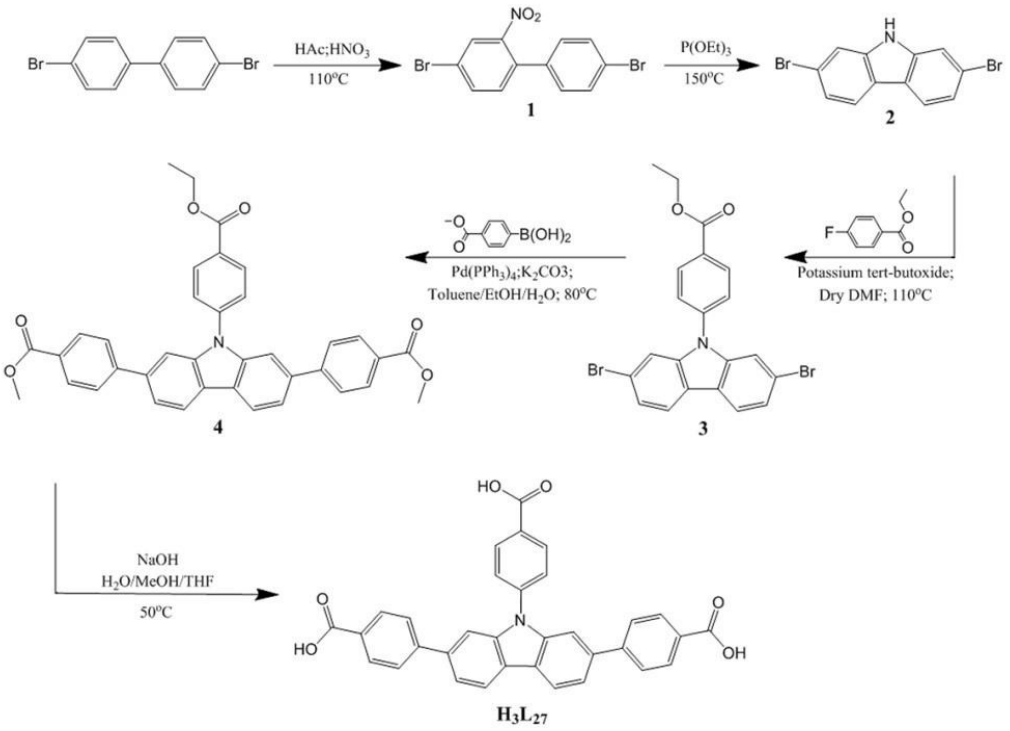

Scheme 1. Synthesis of 2, 7-bis(4-benzoic acid)-N-(4-benzoic acid) carbazole **(H_3L_{27})**

132.05, 129.42, 127.29, 123.09, 121.85. MS (EI): calculated for $C_{12}H_7Br_2NO_2$ m/z: 357.00, found m/z: 356.90.

2,7-Dibromocarbazole(2): Compound **2** was synthesized followed the reported procedure.[42] A solution of **1** (10 g, 28.0 mmol) in phosphorous acid triethyl ester (35 ml) was heated to 150°C in an inert atmosphere. The system was allowed to react for 18 h and a brown solution was obtained. The solvents were removed by vacuum distillation and the product was purified by column chromatography with petroleum ether/ethyl acetate (10:1, v/v) as the eluent. The title compound was obtained as white crystal (4.82 g, 53% yield). ^{1}H NMR (400 MHz, acetone- d_6): δ (ppm) = 10.63 (s, 1 H), 8.06 (d, *J* = 8.36 Hz, 2 H), 7.74 (d, *J* = 1.52 Hz, 2 H), 7.36 (dd, *J* = 1.56, 6.76 Hz, 2 H). ^{13}C NMR (400 MHz, acetone- d_6): δ (ppm) = 141.12, 122.43, 121.75, 121.61, 119.10, 114.04. MS (EI): calculated for $C_{12}H_7Br_2N$ m/z: 325.00, found m/z: 325.10.

2,7-Dibromo-N-(4-ethyl benzoate) carbazole (3): Potassium tert-butoxide (3.36 g, 30 mmol) and 2,7-Dibromocarbazole (9.78 g, 30 mmol) were dissolved in dry DMF (300 mL) in a two-necked flask fitted with a magnetic stirrer and condenser. Under an atmosphere of nitrogen, the solution was stirred at 110 °C for 60 min and then ethyl 4-fluorobenzoate (6.10 ml, 33 mmol) was added. The system was allowed to react for 24 h and an apricot solution was obtained. The solvents were then removed by vacuum distillation. The crude residue was recrystallized from ethanol (50 ml). A white powder was obtained (10.7 g, 88.6% yield). ^{1}H NMR (400 MHz, $CDCl_3$) δ (ppm) = 8.35 (d, *J* = 8.5 Hz, 2H), 7.97 (d, *J*= 8.3 Hz, 2H), 7.64 (d, *J* = 8.5 Hz, 2H), 7.56 (d, *J* = 1.56 Hz, 2H), 7.45 (dd, *J* = 1.6, 6.7 Hz, 2H), 4.49 (q, *J* = 7.1 Hz, 2H), 1.48 (t, *J* = 7.1 Hz, 3H). ^{13}C NMR (400 MHz, $CDCl_3$) δ (ppm) = 165.64, 141.30, 140.50, 131.67, 130.08, 126.52, 124.16, 122.02, 121.60, 113.03, 61.43, 14.30. MS (EI): calculated for $C_{21}H_{15}Br_2NO_2$ m/z: 473.16, found m/z: 473.06

2,7-bis(4-methyl benzoate)-N-(4-ethyl benzoate) carbazole (4): A solution of Methyl 4-boronobenzoate (2.17 g, 12 mmol) and K_2CO_3 (38.8 g, 0.28 mol) in 1:1 EtOH/H_2O (80 ml) was added to a solution of 2,7-Dibromo-N-(4-methyl benzoate) carbazole (2.51 g, 5.3 mmol) in toluene (80 ml). The reaction was stirred for 20 min and then tetrakis(triphenylphosphine) palladium(0) (0.30 g, 0.26 mmol) was added as catalyst. The suspension was refluxed under nitrogen for 5 days. The reaction mixture was allowed to cool to room temperature and the solid in the reaction mixture was removed by filtration. The filtrate was extracted with ethyl acetate and the solvent in the collected organics was removed under reduced pressure. After recrystallization from ethanol, 2,7-bis(4-methyl benzoate)-N-(4-methyl benzoate) carbazole was obtained as white solid (1.98 g, yield 64%). ^{1}H NMR (400 MHz, DMSO-d_6) δ (ppm) = 8.41 (d, *J* = 8.2 Hz, 2 H), 8.29 (d，*J* = 8.5 Hz,2 H),8.04 (d, *J* = 8.4 Hz,4 H), 7.98 (d, *J* = 8.5 Hz, 2 H), 7.90(d, *J* = 8.3 Hz, 4 H), 7.72 (d, *J* = 9.3 Hz, 2 H), 7.60 (dd, *J* = 2.8, 5.6 Hz, 2 H), 4.34 (d, *J* = 7.1 Hz,2 H), 2.81 (s, 2 H) 1.34 (d, *J* = 7.1 Hz,3 H). ^{13}C NMR (400 MHz, DMSO-d_6) δ (ppm) = 166.06, 162.78, 145.69, 141.16, 140.01, 137.89, 131.83, 130.32, 129.36, 128.31, 127.76, 127.26, 126.21, 123.53, 121.86, 108.62, 61.21, 36.25, 31.23, 14.67. MS (EI): calculated for $C_{37}H_29NO_6$ m/z: 583.64, found m/z: 583.63.

2,7-bis(4-benzoic acid)-N-(4-benzoic acid) carbazole (H_3L_{27}): A solution of NaOH (1.20 g, 30 mmol) in H_2O (15 ml) was added in a suspension of 2,7-bis(4-methyl benzoate)-N--(4-methyl benzoate) carbazole (1.98 g, 3.39 mmol) in 1:1 methanol/tetrahydrofuran (15 ml). The mixture was stirred at

Table 1 Crystal and X-ray experimental data for compounds **TCZ-001** – **TCZ-005**

Compound	TCZ-001	TCZ-002	TCZ-003	TCZ-004	TCZ-005
Empirical formula	$C_{90}H_{98}N8O_{22}Zn_3$	$C_{94}H_{102}N_8O_{20}Zn_3$	$C_{91}H_{94}N_8O_{19}Zn_3$	$C_{90}H_{94}Cd_3N_8O_{20}$	$C_{278}H_{284}Cd_9N_{25}O_{66.5}$
Formula weight	1839.87	1860.02	1799.85	972.47	6051.04
Crystal system	Triclinic	Monoclinic	Triclinic	Triclinic	Monoclinic
Space group	P-1	C2/c	P-1	P-1	Pn
a(Å)	14.6832(5)	30.057(6)	14.8042(4)	11.151(4)	15.8325(19)
b(Å)	15.5902(6)	16.187(3)	16.9788(4)	14.724(5)	22.884(3)
c(Å)	19.3560(3)	21.894(4)	17.5636(6)	15.569(5)	36.596(5)
α(°)	83.727(5)	90	99.169(2)	63.180(12)	90
β(°)	81.479(5)	114.478(3)	104.186(3)	71.118(14)	97.523(2)
γ(°)	87.507(6)	90	101.157(2)	79.302(17)	90
V(Å^3)	4354.0(2)	9695(3)	4098.8(2)	2156.1(12)	13145(3)
Z	2	4	2	2	2
Temperature(K)	293(2)	293(2)	293(2)	293(2)	293(2)
D_c(Mg m^{-3})	1.403	1.274	1.458	1.498	1.509
μ(mm^{-1})	0.898	0.784	1.672	0.809	0.799
F(000)	1920	2912	1876	994	6094
R_1[a],wR2b(I>2σ(I))	0.0780,0.2223	0.0495,0.1450	0.0736, 0.2125	0.0429,0.1379	0.0519,0.1315
θ_{range}(deg)	2.00 to 27.45	2.25 to 27.48	3.36 to 74.66	2.11 to 27.52	2.20 to 27.51
h,k,l ranges	-17 to 19	-32 to 38	-18 to 17	-14 to 14	-20 to 20
	-20 to 19	-21 to 20	-21 to 14	-16 to 19	-29 to 29
	-25 to 25	-28 to 28	-21 to 21	-19 to 20	-47 to 47
GOF on F2	1.020	1.089	1.099	1.048	1.107

[a] $R = \sum||F_O| - F_C||/\sum|F_O|$. [b] $wR_2 = [P[w(F_O^2 - F_C^2)^2]/\sum[(F_O^2)^2]]^{1/2}$.

View Article Online
DOI: 10.1039/C7CE00361G

50 °C for overnight and then it was added to a solution of HCl (300 ml, pH= 2). After stirring for 10min, sediment was collected by filtration. Washed with tetrahydrofuran and ether and then allowed to dry under reduced pressure, a beige solid was obtained (1.70 g, yield 95%). ^{1}H NMR (400 MHz, DMSO-d_6) δ (ppm) = 8.45 (d, *J* = 8.1 Hz, 2 H), 8.28 (d，*J* = 8.5 Hz, 2 H),8.03 (d, *J* = 8.4 Hz, 4 H), 7.95 (d, *J* = 8.5 Hz, 2 H), 7.89 (d, *J* = 8.4 Hz, 4 H), 7.74 (d, *J* = 8.9 Hz, 2 H), 7.62 (dd, *J* = 7.0, 12.1 Hz, 2 H). ^{13}C NMR (400 MHz, DMSO-d_6) δ (ppm) = 167.64, 167.21, 145.28, 141.41, 140.89, 138.31, 132.00, 130.45, 129.97, 129.30, 127.75, 127.23, 123.18, 122.07, 120.71, 108.66. MS (EI): calculated for $C_{33}H_{21}NO_6$ m/z: 526.14, found m/z: 526.13.

Synthesis of $[Zn_3(L_{27})_2(DMA)_6(H_2O)_4]_n$ (TCZ-001)

Solvothermal reaction of $Zn(NO_3)_2{\cdot}6H_2O$ (59.5 mg, 0.2 mmol), 2,7-bis(4-benzoic acid)-N-(4-benzoic acid) carbazole (**H_3L_{27}**) (26.3 mg, 0.05 mmol) in the mixture of N,N'-dimethylacetamine (DMA) (1.5 ml) and H_2O (0.5 ml) at 353 K for 72 h gave rise to colorless prism crystals of **TCZ-001** (18.5 mg, Yield: 40.3%). Anal. Calcd (%) for $C_{90}H_{98}N_8O_{22}Zn_3$: C 58.75, H 5.36, N 6.09. Found: C 58.93, H 5.12, N 5.99.

Synthesis of $[Zn_3(L_{27})_2(DMA)_6(CH_3CH_2OH)_2]_n$ (TCZ-002)

Solvothermal reaction of $Zn(NO_3)_2{\cdot}6H_2O$ (59.5 mg, 0.2 mmol), 2,7-bis(4-benzoic acid)-N-(4-benzoic acid) carbazole (**H_3L_{27}**) (26.3 mg, 0.05 mmol) in the mixture of N,N'-dimethylacetamine (DMA) (1.5 ml) and ethanol (0.5 ml) at 353 K for 72 h gave rise to apricot bulk crystals of **TCZ-002** (22.1 mg, Yield: 47.6%). Anal. Calcd (%) for $C_{94}H_{102}N_8O_{20}Zn_3$: C 60.70, H 5.53, N 6.02. Found: C 60.08, H 5.61, N 6.07.

Synthesis of $[Zn_3(L_{27})_2(DMA)_6(CH_3OH)]_n$ (TCZ-003)

Solvothermal reaction of $Zn(NO_3)_2{\cdot}6H_2O$ (59.5 mg, 0.2 mmol), 2,7-bis(4-benzoic acid)-N-(4-benzoic acid) carbazole (**H_3L_{27}**) (26.3 mg, 0.05 mmol) in the mixture of N,N'-dimethylacetamine (DMA) (1.5 ml) and methanol (0.5 ml) at 353 K for 72 h gave rise to colorless bulk crystals of **TCZ-003** (23.7 mg, Yield: 52.7%). Anal. Calcd (%) for $C_{91}H_{94}N_8O_{19}Zn_3$: C 60.72, H 5.26, N 6.22. Found: C 59.92, H 5.11, N 6.03.

Synthesis of $[Cd_3(L_{27})_2(DMA)_6(H_2O)_2]_n$ (TCZ-004)

Solvothermal reaction of $Cd(NO_3)_2{\cdot}6H_2O$ (61.7 mg, 0.2 mmol), 2,7-bis(4-benzoic acid)-N-(4-benzoic acid) carbazole (**H_3L_{27}**) (26.3 mg, 0.05 mmol) in the mixture of N,N'-dimethylacetamine (DMA) (1.5 ml) and 10:1 ethanol/H_2O (0.5 ml) at 373 K for 96 h gave rise to colorless bulk crystals of **TCZ-004** (15.3 mg, Yield: 31.5%). Anal. Calcd (%) for $C_{90}H_{94}N_8O_{20}Cd_3$: C 55.57, H 4.87, N 5.76. Found: C 55.31, H 4.81, N 5.61.

Synthesis of $[Cd_9(L_{27})_6DMA_{13}(4,4'\text{-BPY})_2(OH)_2(H_2O)_{13.5}]_n$ (TCZ-005).

The synthesis of **TCZ-005** was carried out by heating a solution mixture of 2,7-bis(4-benzoic acid)-N-(4-benzoic acid) carbazole (**H_3L_{27}**) (26.3 mg, 0.05 mmol), 4,4'-bipyridine (7.8 mg, 0.05 mmol) and $Cd(NO_3)_2{\cdot}6H_2O$ (61.7 mg, 0.2 mmol) in N,N'-dimethylacetamine (DMA) (1.5 ml) and H_2O (0.5 ml) at 353 K for 72 h. Daffodil prism crystals of **TCZ-005** were obtained (47 mg, Yield: 48 %). Anal. Calcd (%) for $C_{556}H_{552}N_{50}O_{124}Cd_{18}$: C 55.92, H 4.66, N 5.86. Found: C 55.41, H 4.62, N 5.63.

Single-Crystal Structure Determination.

The X-ray single-crystal structure analyses for the **TCZ-001**, **TCZ-002**, **TCZ-004**, **TCZ-005** were collected on a Rigaku Saturn 724HG CCD diffractometer (Mo Kα radiation λ=0.71073Å graphite-monochromator) at 293(2) K. **TCZ-003** was performed on a SuperNova, Dual, Cu at zero, Atlas diffractometer equipped with graphite-monochromated Cu Ka radiation (λ= 1.54184 Å) at 293(2) K. All of the structure were solved by direct methods and refined by full matrix least-squares of F^2 using the SHELX-97 program.[48] Hydrogen atoms were added in idealized positions. The SQUEEZE routine of the PLATON software suite was used in removing highly disordered solvent molecules in **TCZ-002** and **TCZ-005**. The final formulas were calculated according to the Squeeze results combined with the results from elemental analyses and thermogravimetric analysis (TGA).[49,50] Crystal data for **TCZ-001** - **TCZ-005** are presented in **Table 1**. Selected bond lengths and angles of **TCZ-001** – **TCZ-005** are listed in **Table S1** of Supporting Information.

Experiments of metal ion sensing

The finely ground powder samples (3 mg, respectively) immersed in 3 mL DMA, H_2O or ethanol solutions of $M(NO_3)_x$. Suspension solutions were obtained after preparation by an ultrasound method for 3 hours at room temperature. And then, the luminescence emission spectra of the suspension solutions were measured immediately under excitation at 370nm. The data were obtained from two measurements on independent luminescence sensing experiments.

Photophysical measurements

The solid-state and suspension solutions luminescence emission/excitation spectra and solid-state luminescence lifetimes were recorded on an Edingburgh Insruments FLS980 fluorescence spectrophotometer. The quantum yields of the solid-state samples were determined by an absolute method using an integrating sphere on an Edingburgh Insruments FLS920 spectrometer. The lifetimes of the solid-state samples were acquired on an Edinburgh Analytical FLS920 instrument with a Picoseconds Laser Diode.

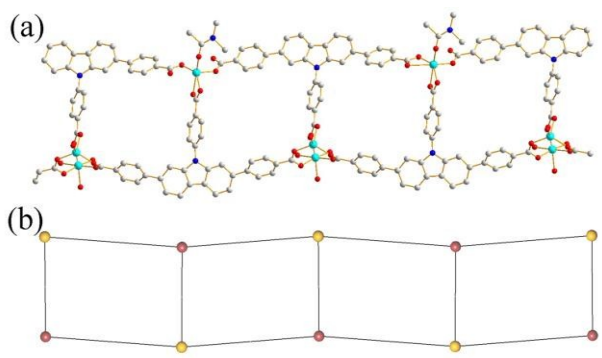

Fig. 1 (a) View of the 1D infinite chain in **TCZ-001**; (b) Topological representation of the chain in **TCZ-001** (ligand **L_{27}** are marked as yellow balls; metal nodes are marked as plum ball.

View Article Online
DOI: 10.1039/C7CE00361G

Results and discussion

Crystal structure of TCZ-001

Single crystal X-ray diffraction analysis indicates that TCZ-001 crystallizes in the triclinic $P\bar{1}$ space group. Structural analysis of **TCZ-001** shows that it is one-dimensional (1D) two-connected-chained structure. The T-shape $\mathbf{L_{27}}$ ligand is connected by dinuclear Zn^{II} cluster and mononuclear Zn^{II} ion which coordinated on one of the two connected chains respectively (Fig 1a). The dinuclear Zn^{II} cluster contains two types of Zn^{II} ion in different coordination modes (Fig. S1b). One of the two types of $Zn^{II}(1)$ is coordinated to three O atoms from the carboxylate group of three $\mathbf{L_{27}}$ ligands and an O atom from a water molecule. The other one $Zn^{II}(3)$ is coordinated to three O atoms from the carboxylate group of same three $\mathbf{L_{27}}$ ligands and it is coordinated to three O atoms from three water molecules at the same time. In the meantime, it is the key for forming crystal that forming hydrogen bond between H atoms of coordinated water molecules and O atoms belonged to other chains. The mononuclear $Zn^{II}(2)$ ion on the other chain is five-connected with oxygen atoms of carboxylate group from three $\mathbf{L_{27}}$ ligands and the last coordination position is occupied by a DMA molecule (Fig. S1a). As summarized in **Table S1**, the Zn-O bond lengths of **TCZ-001** range from 1.926(3) Å to 2.193(3) Å.

A PLATON calculation indicated that the total potential solvent volume when the DMA molecules are removed is 1711.8 $Å^3$, which corresponds to 39.30% (4354.0 $Å^3$) totally volume. Topologically, dinuclear Zn^{II} cluster , mononuclear Zn^{II} ion and $\mathbf{L_{27}}$ ligands are regarded as 3-connected nodes, the network of **TCZ-001** is classified as 3-connected uninodal $\{4^2.6\}$ topology (Fig. 1b).

Crystal structure of TCZ-002

Structural analysis according to single crystal X-ray diffraction indicates **TCZ-002** crystallizes in the monoclinic *C2/c* space group. A typical trinuclear Zn^{II} cluster is connected by $\mathbf{L_{27}}$ ligands and a three-dimensional (3D) porous structure is obtained. The asymmetric unit possesses one $\mathbf{L_{27}}$ ligands, half of a three Zn^{II} cluster and a DMA molecule. The Zn^{II} cluster consists of two tetrahedral Zn^{II} ions [$Zn^{II}(2)$, $Zn^{II}(2')$] and an octahedral Zn^{II} ion [$Zn^{II}(1)$] (Fig 2a). $Zn^{II}(1)$ is six-coordinated by six carboxyl oxygen atoms of six $\mathbf{L_{27}}$ ligands. Both $Zn^{II}(2)$ and $Zn^{II}(2')$ are bonded to a DMA molecule and three bismonodentate carboxylates, which are also bonded to $Zn^{II}(1)$. The $Zn^{II}(1)$-O bond lengths vary from 2.0198(17) Å to 2.094(2) Å and the $Zn^{II}(2)/(2')$-O bond lengths range from 1.9455(19) Å to 1.997(2) Å. A 1D channel in **TCZ-002** has a diameter of 7.4 Å and the solvent-accessible volume is 1074.0 $Å^3$, which is 44.3% of per unit cell volume (2423.8 $Å^3$) as calculated by PLATON (Fig 2b, 2c). According to the data of TGA from 303 K to 413 K, free solvent molecules occupy 24% of total weight of **TCZ-002**.

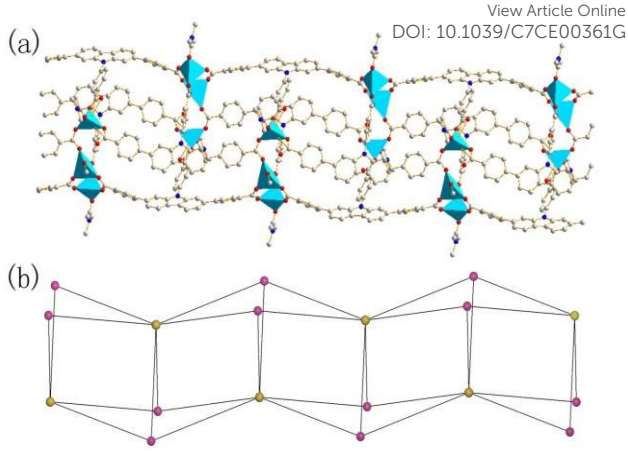

Fig. 3 (a) View of the 1D infinite chain in **TCZ-003**; (b) Topological representation of the chain in **TCZ-003** (ligand $\mathbf{L_{27}}$ are regarded as pink balls; metal nodes are marked as yellow ball).

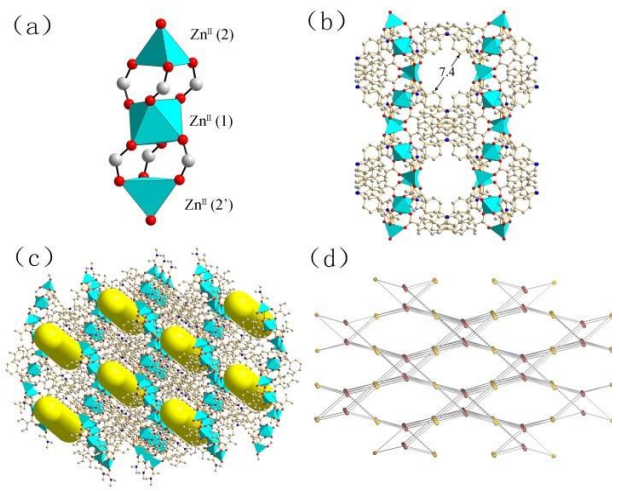

Fig. 2 (a) Secondary building units (SBUs) of **TCZ-002**; (b) 3D framework of **TCZ-002** having a diameter of 7.4 Å; (c) View of 1D channel indicated by a yellow cylinder; (d) Schematic view of the 3,6-connected network in **TCZ-002**.

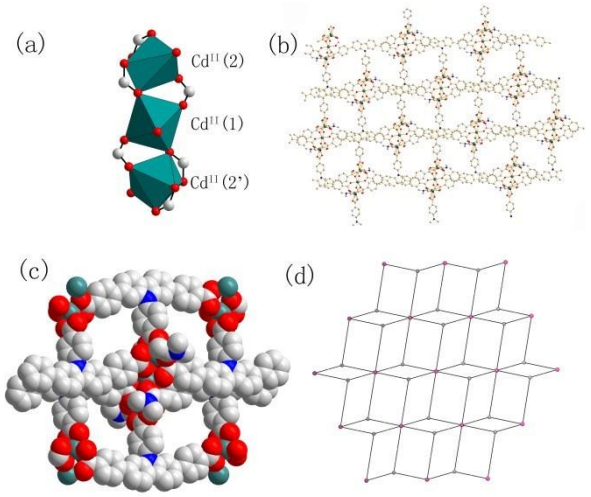

Fig. 4 (a) Secondary building units (SBUs) of **TCZ-004**; (b) 2D structure of **TCZ-004** viewed down the c-axis with a 11.6 x 8.36 Å channel. (c) A space-filling version of the 2D network of **TCZ-004**. (d) Topological representation of the 3,6-connected network in **TCZ-004**.

View Article Online DOI: 10.1039/C7CE00376C

And there are ca.238 electron count voids and 1090 total potential solvent accessible void volume in per unit cell as calculated by PLATON. So it can be figured out that there are three and a half DMA molecules and two ethanol molecules per unit cell. From a topological point of view, the Zn^{II} cluster could be regard as 6-connected node and the $\mathbf{L_{27}}$ ligands could be regard as 3-connected node. TOPOS analysis based on that view reveals that the 3D structure of **TCZ-002** can be rationalized to a 3,6-connected net with a point symbol of $\{4^{2\cdot}6\}_2\{4^{4\cdot}6^{2\cdot}8^{7\cdot}10^2\}$ (Fig 2d).

Crystal structure of TCZ-003

Single crystal X-ray diffraction analysis proves that **TCZ-003** crystallizes in the triclinic $P\bar{1}$ space group and it is also 1D structure, however, which is different from the 1D structure of **TCZ-001**. The difference in the structure between **TCZ-003** and **TCZ-001** is that **TCZ-003** is 1D four-connected-chained structure and the $\mathbf{L_{27}}$ ligands are connected by trinuclear Zn^{II} clusters (Fig. 3a). Meanwhile, the asymmetric unit of **TCZ-003** consists of a trinuclear Zn^{II} cluster, two $\mathbf{L_{27}}$ ligands, six DMA molecules and a coordinated methanol molecules. $Zn^{II}(1)$ of the trinuclear Zn^{II} clusters are four coordinated with O atoms from three carboxyl groups of $\mathbf{L_{27}}$ ligands and a DMA molecules, including an O atom from a carboxyl group which is the bridge between $Zn^{II}(1)$ and $Zn^{II}(3)$. $Zn^{II}(3)$ and $Zn^{II}(2)$ are bridged by three carboxyl groups of $\mathbf{L_{27}}$ ligands (Fig. S2). In addition, $Zn^{II}(3)$ is coordinated with a methanol molecule and $Zn^{II}(2)$ is coordinated with a DMA molecule. The Zn-O bond distances are range from 1.933(4) Å to 2.049(4) Å. The solvent-accessible volume is 30.90% (1265.6 $Å^3$/4098.8$Å^3$) as calculated by PLATON when the solvent molecules are removed. The structure of **TCZ-003** can be described as a 3, 6-connected network with a Schläfli symbol of $\{4^{11}.6^4\}\{4^3\}_2$when each twisty trinuclear Zn^{II} cluster is regarded as 6-connected node and each $\mathbf{L_{27}}$ ligand is reduced as a 3-connected node by TOPOS software (Fig. 3b).

Crystal structure of TCZ-004

According to single crystal X-ray diffraction analysis, **TCZ-004** possesses a two-fold two-dimensional (2D) network that crystallizes in the triclinic $P\bar{1}$ space group. The framework is electrically neutral and contains a linear three-Cd^{II} cluster connected by sixteen carboxylate oxygens of six $\mathbf{L_{27}}$ ligands and four DMA molecules (Fig. 4a, 4b, 4c). In the linear three-Cd^{II} cluster, $Cd^{II}(2)$ and $Cd^{II}(2')$ are six connected by O atoms from three $\mathbf{L_{27}}$ ligands and a DMA molecule. Similar to $Cd^{II}(2)$ and

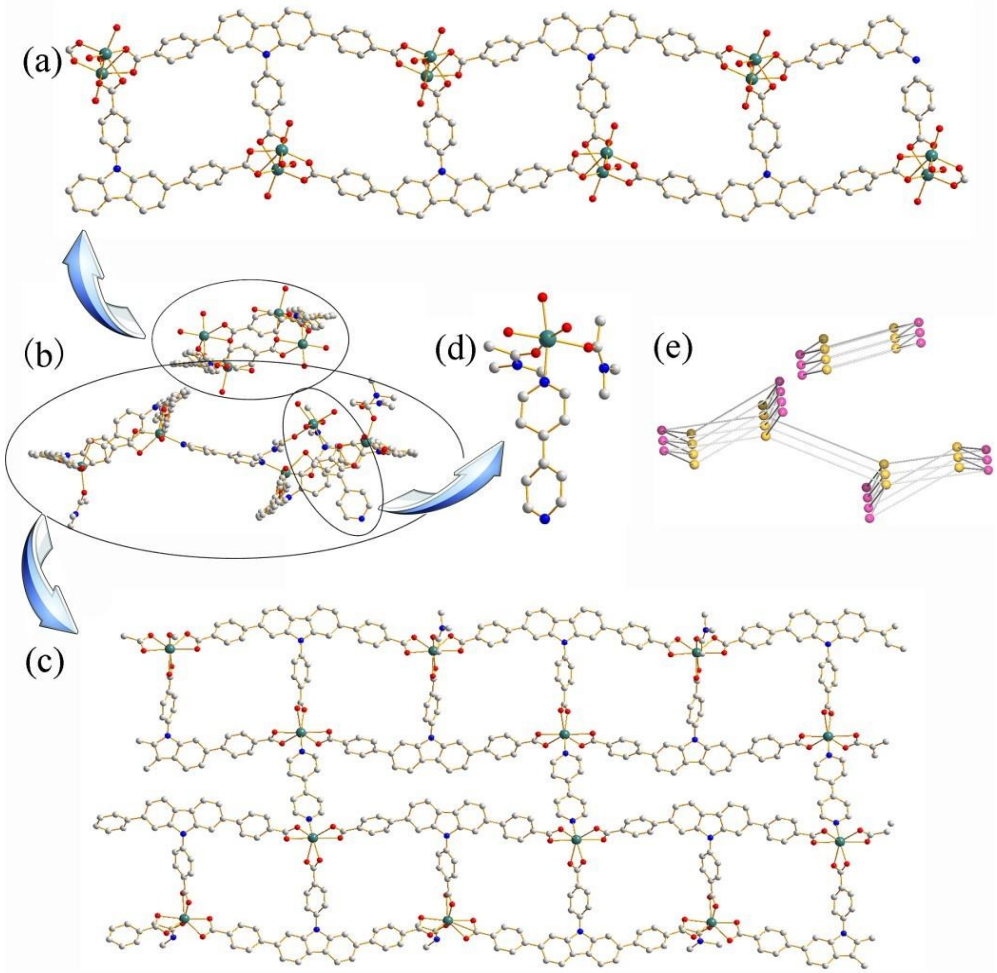

Fig. 5 (b) View of the 1D infinite chain in **TCZ-005** down the b-axis and (a), (d), (c) are the view of parts of **TCZ-005** down the c-axis. (e) Topological representation of the chain in **TCZ-005**.

View Article Online
DOI: 10.1039/C7CE00361G

Cd^{II}(2'), Cd^{II}(1) is also six coordinated with O atoms, but which are from four $\mathbf{L_{27}}$ ligands and two DMA molecules. The range of Cd-O bond lengths is from 2.167(2) Å to 2.376(3) Å and the void volume calculated by PLATON is 22.1% of total volume of the framework. Topologically, the linear three-Cd^{II} cluster can be viewed as a 6-connected node, therefore, the network of **TCZ-004** belong to a 3,6-connected net with a Schläfli symbol of $\{4^3\}_2.\{4^6.6^6.8^3\}$ (Fig. 4d).

Crystal structure of TCZ-005

Single-crystal X-ray diffraction of **TCZ-005** revealed that the framework belong to the Monoclinic *Pn* space group and the huge asymmetric unit consists of nine Cd^{II} ions, six $\mathbf{L_{27}}$ ligands, thirteen DMA molecules, two 4,4'-Bipyridine molecules, thirteen and a half H_2O molecules and two hydroxide ions. **TCZ-005** is composed of three types of parallel 1D structure chains (Fig. 5b). Two types of the chains are formed by connecting mononuclear Cd^{II} ion with $\mathbf{L_{27}}$ ligands and both of them are bridged by 4,4'-bipyridine molecules(Fig. 5c). The other type of chain consists of dinuclear Cd^{II} cluster connected by $\mathbf{L_{27}}$ ligands and forming hydrogen bond between H atoms of coordinated water molecules and O atoms belonged to other chains results in the growth of the crystal (Fig. 5a). The Cd-O bond distances are range from 2.169(4) Å to 2.631(6) Å and Cd-N bond distances are from 2.295(7) Å to 2.321(5) Å which are shown in **Table S1**. The solvent-accessible volume is 28.70% as calculated by PLATON, which is limited as part of the channels of **TCZ-005** are occupied by $[Cd(OH)_2(DMA)_2(4,4'\text{-Bipyridine})(H_2O)]$ cluster (Fig. 5d). Topologically, the chains consists of dinuclear Cd^{II} cluster belong to 3-connected net with a Schläfli symbol of $\{4^2.6\}$ and the chains connected by 4,4'-Bipyridine has a point (Schläfli) symbol $\{4^{2\cdot}6^{3\cdot}8\}\{4^{2\cdot}6\}_3$. The structure of **TCZ-005** could be described as a SP 1-periodic net (4,4)(0,2) in the 1D_2D.ttd database (Fig. 5e).

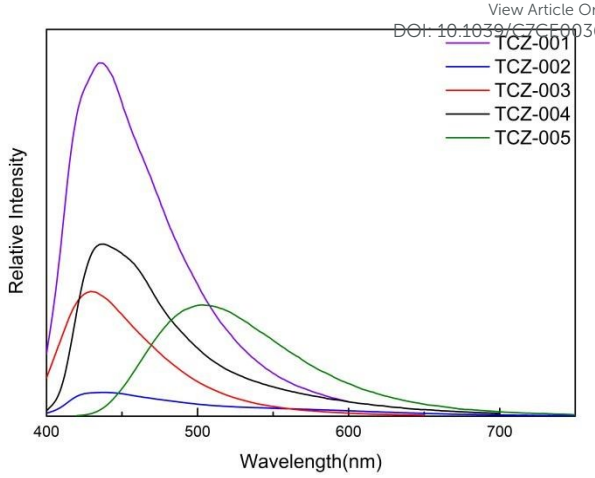

Fig. 6 Solid-state emission spectra of **TCZ-001** to **TCZ-005**.

X-ray powder diffraction and thermal analysis

Powder X-ray diffraction (PXRD) for the bulk samples of **TCZ-001** – **TCZ-005** were carried out at room temperature. For **TCZ-001** to **TCZ-005**, the experimental PXRD patterns correspond well with the simulated from the data of single crystal X-ray diffraction and are shown in Fig. S3. To estimate the thermal stability, thermogravimetric analysis (TGA) experiments were

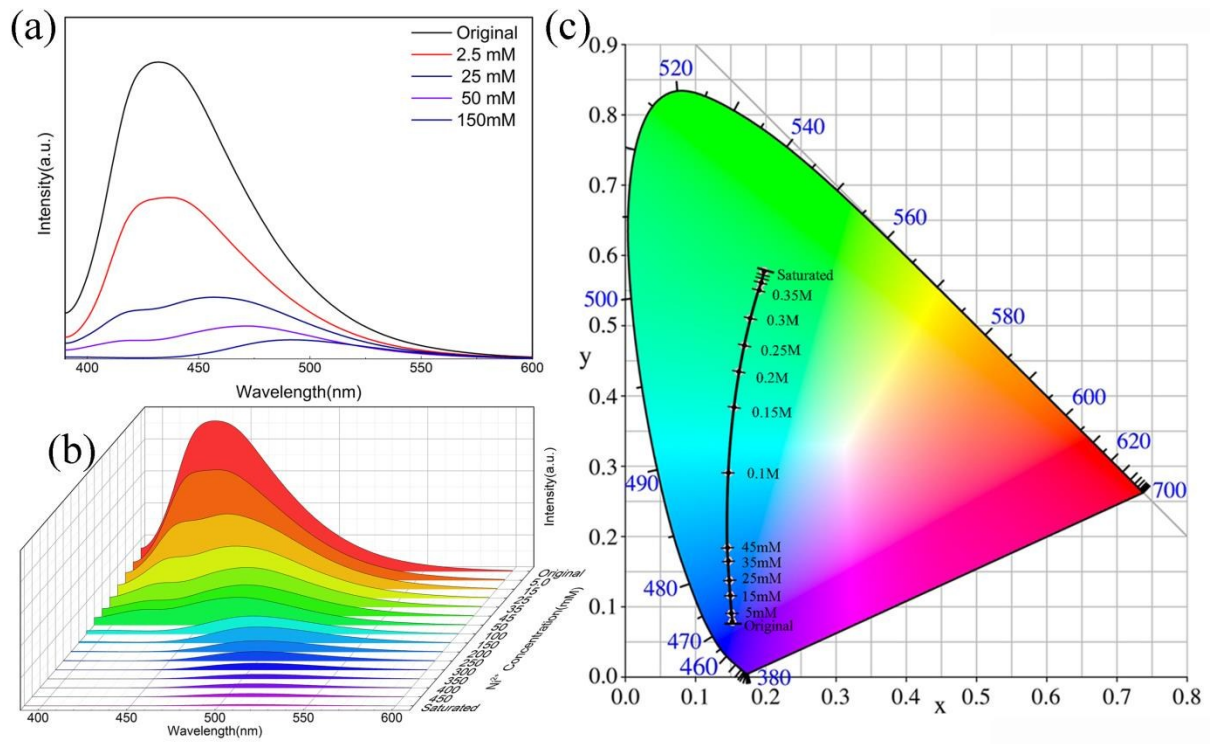

Fig. 7 (a) and (b) Emission spectra of **TCZ-001** in DMA solution upon the addition of various concentrations of Ni^{2+}; (c) CIE chromaticity diagram showing the Ni^{2+} concentration-dependent luminescence colour change of **TCZ-001** in DMA solution under the excitation at 370nm.

View Article Online
DOI: 10.1039/C7CE00356C

performed on polycrystalline samples of **TCZ-001** to **TCZ-005** under a N_2 atmosphere with a heating rate of 10 °C min^{-1} in the range of 30-800 °C. For **TCZ-001**, a weight loss of 23.5% from room temperature to 140 °C is ascribed to the loss of free DMA molecules (calc. 23.6%). From 150 to 400 °C, coordinated DMA and water molecules were removed generally with a weight loss of 9.8% (calc. 8.7%). The frame work collapses and decomposes after 420 °C. Similar to **TCZ-001**, the curves of **TCZ-002** to **TCZ-005** display weight losses of 23.8%, 20.1%, 19.9% and 18.4%, respectively, corresponding to the removal of guest DMA, water, ethanol or methanol molecules (calc. 23.6%, 19.4%, 19.7% and 16.0%). The coordinated DMA, water molecules or methanol molecules were removed slowly from 150 to 370 °C. Upon further heating, the TG curves of **TCZ-004** and **TCZ-005**, which assembled from $\mathbf{L_{27}}$ ligands and Cd^{II} ions, display rapid weight losses from 380 to 420 °C. Comparing to **TCZ-004** and **TCZ-005** in the TG curve, **TCZ-001**, **TCZ-002** and **TCZ-003**, which contain Zn^{II} ions, are more stable and the weight losses are observed from 420 to 495 °C. All of the TGA curves are shown in Fig. S4.

Photoluminescence properties

The photoluminescence properties of **TCZ-001** to **TCZ-005** and $\mathbf{H_3L_{27}}$ ligand were investigated under room temperature. The free solid-state H_3L_{27} ligand show a blue fluorescent emission band at 459 nm under 375 nm wavelength excitation, which is probably due to $\pi^* \rightarrow n$ or $\pi^* \rightarrow \pi$ transitions.[51-58] Under excitation at 370 nm, the solid-state emission spectra of **TCZ-001** to **TCZ-005** display intense emission bands centered at 435 nm, 435 nm, 430 nm, 438 nm and 500 nm respectively. The blue shifts of TCZ-001 to TCZ-004 are tentatively assigned strong electrostatic interaction between the L_{27} ligands and metal ions by donation of the lone pair electrons of O atoms to the empty orbitals of the metal ions.[51,57,61] The emissions of **TCZ-001** to **TCZ-004** are neither metal-to-ligand charge transfer (MLCT) nor ligand-to-metal charge transfer (LMCT) in nature since Zn^{II}/Cd^{II} ions are difficult to oxidize or to reduce due to their d^{10} configurations. For TCZ-005, the emission may exist as a mixture characteristic of intraligand and ligand-to-ligand charge transitions (LLCT), since the Cd^{II} ions are difficult to oxidize or reduce due to their d^{10} configurations.[51,52,58,61,62] The emission decay lifetimes of **TCZ-001** to **TCZ-005** were found to be $\tau_{TCZ-001}$ = 2.690 ns, $\tau_{TCZ-002}$ = 4.352 ns, $\tau_{TCZ-003}$ = 3.453 ns, $\tau_{TCZ-004}$ = 2.572 ns and $\tau_{TCZ-005}$ = 64.16 ns. And the emission decay lifetimes of $\mathbf{H_3L_{27}}$ was τ_{H3L27} = 3.78 ns. The external quantum yield (Φ_F) of **TCZ-001** is as high as 25.95%, a remarkable enhancement of the luminescent quantum yield compared with the solid-state emission of $\mathbf{H_3L_{27}}$ (Φ_F = 14.3%). However, the external quantum yields of **TCZ-002** to **TCZ-005** were found to be 2.52%, 8.41%, 13.28% and 11.51%, respectively, which were similar or lower than the external quantum yield of the ligand. The different fluorescence intensity for **TCZ-001** to **TCZ-004** is probably due to the different structure of these CPs. In **TCZ-001**, simple 1D polymer chains were confined through hydrogen-bonding interactions and the $\mathbf{L_{27}}$ ligands were in a planar arrangement. While in **TCZ-002**, $\mathbf{L_{27}}$ ligands were connected together to generate a 3D structure and we speculated that a rigid non-planar arrangement due to the coordination of Zn^{II} caused the quenching in emission. The structure of **TCZ-003** is also 1D chain but it is different in emission intensity between TCZ-001 and TCZ-003 may be due to the varying degree of planarity, which will impact the symmetry and the allowance of the lowest energy electronic transitions. In **TCZ-004**, the structure could be regard as a 2D network. And the degree of planarity in **TCZ-004** is better than **TCZ-002** and **TCZ-003**.[51,55,59,63-67]

Metal ion sensing

The intense blue luminescence of **TCZ-001** promotes us to investigate its application in sensing metal ions. The finely ground powder samples (3 mg, respectively) of **TCZ-001** immersed in 3 mL DMA, H_2O or EtOH solutions of $M(NO_3)_x$. Suspension solutions were obtained after preparation by an ultrasound method for 3 hours at room temperature. Although several variations appeared in these suspension solutions, only in solution of Ni^{2+} ions did a remarkable change occur in the emission spectra. The emission spectra of the suspension solutions are shown in Fig. S6. A remarkable red shift in the emission spectra of suspension solution containing Ni^{2+} can be noticed and the distance of the red shift depends on the concentration of Ni^{2+} ions in the suspension solution.

Keeping this in mind, a series of **TCZ-001** suspension solution containing different concentration of Ni^{2+} ion were designed and prepared. As shown in Fig. 7a and Fig. 7b, the main emission peak was gradually moved as the Ni^{2+} concentration increased which can be utilized in selective sensing of Ni^{2+} ions. To facilitate the application of **TCZ-001**, the Ni^{2+} ions concentration-dependent spectra have been transformed into the Commission Internationale de L'Eclairage (CIE) 1931 coordinates and the locus are drawn in the CIE system according to the CIE coordinates (Fig. 7c).[68,69] The

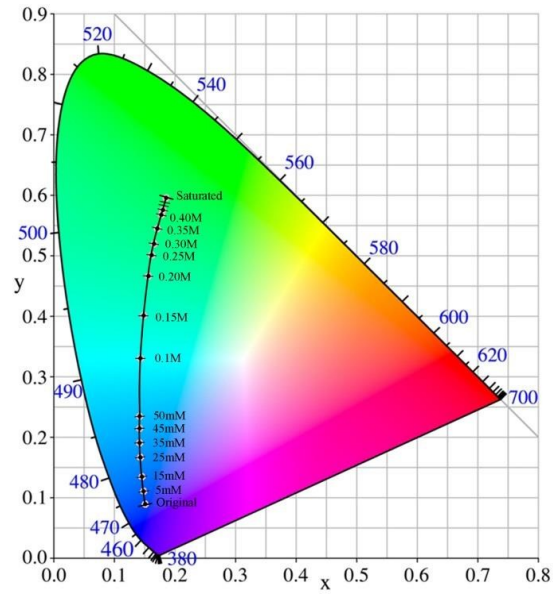

Fig. 8 The locus of **TCZ-003** in CIE chromaticity diagram showing the relationship between luminescence colour and the Ni^{2+} concentration.

View Article Online
DOI: 10.1039/C7CE00361G

coordinates in CIE 1931 are calculated by the ratio between red, green and blue according to emission spectra and it would not be disturbed by the intensity of the excitation light source.[70,71] Thus, the errors, caused by the intensity of the excitation light source or the slit width of the fluorescence spectrometer, can be limited in course of measurement.

With the intention to figure out the reason to the measurement, particles in suspension solutions were separated by centrifugal separation and washed by DMA. After filtering and drying at room temperature, pale green powders were obtained. The Inductively Coupled Plasma OES spectrometer (ICP) data of the pale green powders showed that a partly replacement of Zn^{2+} ions in TCZ-001 by Ni^{2+} ions. (Fig. S7a) Divalent Ni^{2+} cations, which show coordination environment similar to that of Zn^{2+}, may replace partial Zn^{2+} cations during the pre-treatment. Moreover, the partial replacement of the Zn^{2+} was attributed to the strong coordinate ability of Ni^{2+}.[72-75] And the structure of TCZ-001 after measurement is similar to that before measurement, which were monitored by the powder X-ray diffraction (PXRD) (Fig. S7b). In addition, replacing $Zn(NO_3)_2$ by $Ni(NO_3)_2$ in synthesizing **TCZ-001**, light green flocculent precipitate was obtained after solvothermal reaction. Although single crystal cannot be obtained, PXRD show the structure of the flocculent precipitate similar to the structure of **TCZ-001**. And the solid-state emission of the flocculent precipitate is between 430-650nm.(Fig. S8) Thus, we speculate that the emissions between 390 nm to 500 nm are assigned to the CPs with Zn^{2+} nodes and the emissions between 430 nm to 600 nm belong to the CPs with mixture metal nodes including Zn^{2+} and Ni^{2+}. There is a remarkable relationship between the intensity ratios, which is of emissions (390 - 500 nm) to emissions (430 – 600 nm), and percentage composition of the CPs with mixture metal nodes including Zn^{2+} and Ni^{2+}. With the increasing of the CPs with mixture metal nodes including Zn^{2+} and Ni^{2+}, part of the emissions (390 – 500nm) was absorbed by the CPs with mixture metal nodes including Zn^{2+} and Ni^{2+} as excitation light. Meanwhile the percentage compositions of the CPs with mixture metal nodes including Zn^{2+} and Ni^{2+} much depend on the concentration of Ni^{2+} during the measurement.[72-77] Because transmetalation occurred with increasingly concentrated exchange solutions, and less concentrated solutions resulted in exclusively metal sorption, there is evidence that the concentration of the metal ions in the exchange solutions is crucial.[72]

The measurement of Ni^{2+} concentration by **TCZ-001** can also be used in water or ethanol solution (Fig. S9). But the measurement resolution of **TCZ-001** in H_2O or ethanol solution was not as good as that in DMA solution. It might be attributed to the impact to structure of **TCZ-001**, which is caused by the

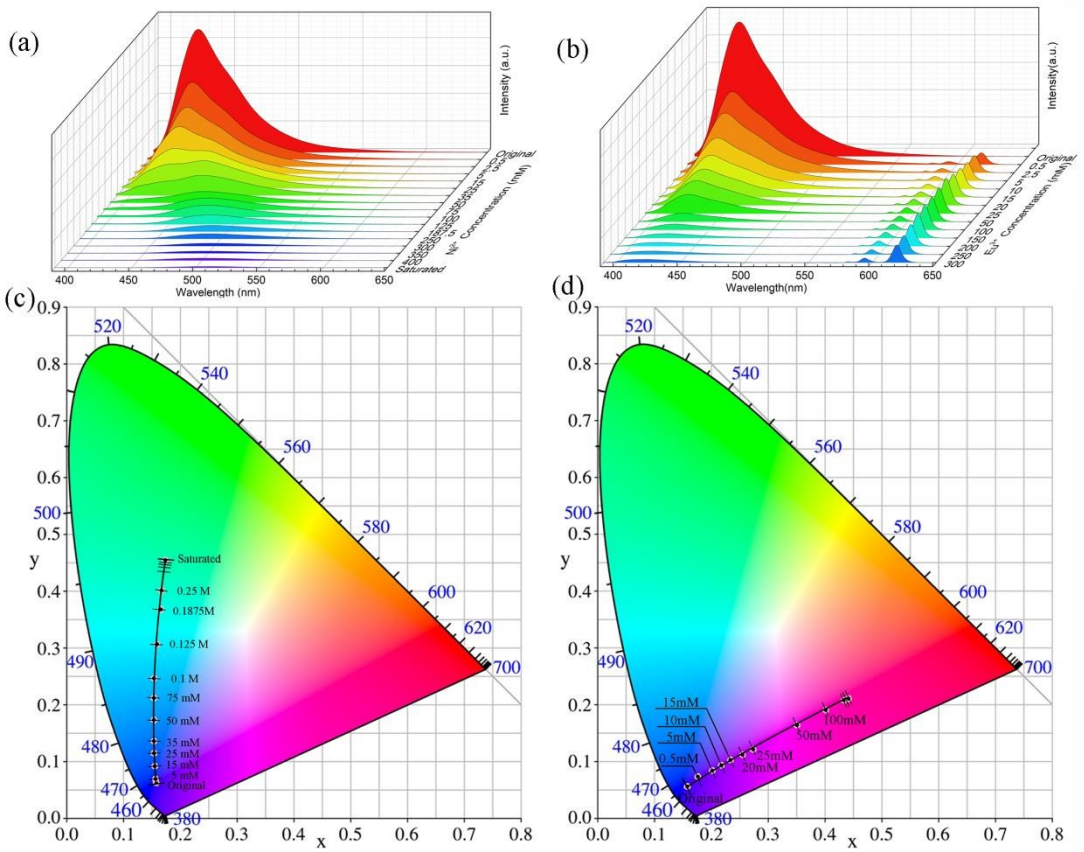

Fig. 9 (a) Emission spectra of **TCZ-004** in DMA solution upon the addition of various concentrations of Ni^{2+}; (b) Emission spectra of **TCZ-004** in DMA solution upon the addition of various concentrations of Eu^{3+}; (c) The relationship of luminescence colour of **TCZ-004** and Ni^{2+} concentration in DMA; (d) The relationship of luminescence colour of **TCZ-004** and Eu^{3+} concentration in DMA.

replacement of DMA molecules in **TCZ-001** by H_2O or EtOH molecules.[78-81]

It was also found in **TCZ-003** and **TCZ-004** that selective sensing of Ni^{2+} ions in DMA solution (Fig. 8, 9c). Comparing with the application of **TCZ-001** and **TCZ-004**, the application of **TCZ-003** has a better resolution in the range of Ni^{2+} concentration less than 0.20 M. But in the range from 0.20 M to 0.35 M, **TCZ-001** performs better than others in resolution. And the measurement of Ni^{2+} concentration by **TCZ-004** was better than the measurement by **TCZ-001** and **TCZ-003** in water or ethanol solution. (Fig. S12) Perhaps it is due to the 2D structure of **TCZ-004**, which is more stable than the 1D structure of **TCZ-001** and **TCZ-003** when the DMA molecules replaced by H_2O or EtOH molecules. Thus, **TCZ-001** and **TCZ-003** might be two potential luminescent probes for detection of Ni^{2+} in DMA. And **TCZ-004** could be used to sense Ni^{2+} concentration in H_2O or EtOH.

In addition to detecting Ni^{2+} concentration, a remarkable phenomenon which exhibits an obvious luminescent and colorimetric response to Eu^{3+} ions in DMA was noticed in the test process by **TCZ-004** (Fig. S11). Moreover, the luminescent and colorimetric response depends on the Eu^{3+} concentration. Therefore, the spectrum of **TCZ-004** with Eu^{3+} was also transformed into the CIE 1931 coordinates (Fig. 9d). It is also found that there is a tiny replacement of Cd^{2+} ions in TCZ-004 by Eu^{3+} ions (Fig. S13a). However, the measurement resolutions of Eu^{3+} concentrations in H_2O or EtOH are too low to be utilized to detect Eu^{3+}. The difference between detecting Ni^{2+} and Eu^{3+} may be tentatively assigned to the size of Eu^{3+} ion and the rate of the transmetalation reactions.

All in all, **TCZ-004** has the potential application as a multiresponsive probe for the detection of the concentration of Ni^{2+} or Eu^{3+} under certain condition.

Conclusions

In summary, five newly porous luminescent coordination polymers based on a novel rigid carboxylate ligand (2,7-bis(4-benzoic acid)-N-(4-benzoic acid) carbazole) have been self-assembled in hydrothermal reaction. **TCZ-001** and **TCZ-003** are 1D infinite linear chain, which show potential as probe materials in selectively and sensitively detecting Ni^{2+} concentration in DMA, H_2O or EtOH solution. Exchanging partial Zn^{2+} cations by Ni^{2+} cations during the pre-treatment can change the colour of the emitting light. The process of detecting Ni^{2+} will not be disturbed by the intensity of the excitation light source or the slit width of the fluorescence spectrometer. **TCZ-002** is a 3D framework with a 1D channel. **TCZ-004** is a 2D layered network and can be used in detecting the concentration of Ni^{2+} in DMA, H_2O or EtOH and Eu^{3+} in DMA solution. **TCZ-005** is a complicated 1D structure which belongs to *Pn* space group. These CPs possibly be utilized as novel porous luminescent material to detecting other diverse metal ion or small molecules. And the applications of these CPs are under investigation in our group.

Acknowledgements

View Article Online
DOI: 10.1039/C7CE00361G

The authors gratefully acknowledge financial support from the National Natural Science Foundation of China (21233009 and 21203194), the 973 program (2014CB845603), the Strategic Priority Research Program of the Chinese Academy of Sciences, Grant No. XDB20000000.

Notes and references

1 X. Sun, Y. Wang and Y. Lei, *Chem. Soc. Rev.*, 2015, **44**, 8019.
2 Z. Hu, B. J. Deibert and J. Li, *Chem. Soc. Rev.*, 2014, **43**, 5815.
3 M. G. Campbell, S. F. Liu, T. M. Swager and M. Dincă, *J. Am. Chem. Soc.*, 2015, **137**, 13780.
4 Y. Guo, X. Feng, T. Han, S. Wang, Z. Lin, Y. Dong and B. Wang, *J. Am. Chem. Soc.*, 2014, **136**, 15485.
5 L.D. Tran, J. Ma, A. G. Wong-Foy and A. J. Matzger. *Chem. Eur. J.*, 2016, **22**, 5509.
6 P.Q. Liao, X.W. Chen, S.Y. Liu, X.Y. Li, Y.T. Xu, M. Tang, Z. Rui, H. Ji, J. P. Zhang and X.M. Chen, *Chem. Sci.*, 2016, **7**, 6528.
7 J. B. DeCoste and G. W. Peterson, *Chem. Rev.*, 2014, **114**, 5695.
8 H. Xu, X.F. Liu, C.S. Cao, B. Zhao, P. Cheng and L.N. He, *Adv. Sci.*, 2016, **3**, 1600048.
9 D. J. Tranchemontagne, J. L. Mendoza-Cortes, M. O'Keeffe and O. M. Yaghi, *Chem. Soc. Rev.*, 2009, **38**, 1257.
10 C Liu and B Yan. Photochem, Photobiol. Sci., 2015, 14, 1644.
11 L. Lu, C. Chen, D. Zhao, J. Sun and X. Yang, *Anal. Chem.*, 2016, **88**, 1238.
12 L. Marciniak and A. Bednarkiewicz, *Phys. Chem. Chem. Phys.*, 2016, **18**, 15584.
13 J. Chen, F. Y. Yi, H. Yu, X. Liu, L. Han and G. Pang, *Eur. J. Inorg. Chem.*, 2016, 3994.
14 L. Z. Yang, J. Wang, A. M. Kirillov, W. Dou, C. Xu, R. Fang, C.L. Xu and W. S. Liu, *CrystEngComm*, 2016, **18**, 6425.
15 P. Silva, S. M. F. Vilela, J. P. C. Tome and F.A. Almeida Paz, *Chem. Soc. Rev.*, 2015, **44**, 6774.
16 A. Douvali, A. C. Tsipis, S. V. Eliseeva, S. Petoud, G. S. Papaefstathiou, C. D. Malliakas, I. Papadas, G. S. Armatas, I. Margiolaki, M. G. Kanatzidis, T. Lazarides and M. J Manos, *Angew. Chem. Int. Ed.,* 2015, **54**, 1651.
17 N. Du, J. Song, S. Li, Y. X. Chi, F. Y. Bai and Y. H. Xing, *ACS Appl. Mater. Interfaces*, 2016, **8**, 28718.
18 W. Liu, X. Huang, C. Xu, C. Chen, L. Yang, W. Dou, W. Chen, H. Yang and W. Liu, *Chem. Eur. J.*, 2016, **22**, 18769.
19 Y. Cui, B. Chen and G. Qian, *Coordin. Chem. Rev.*, 2014, **273–274**, 76.
20 M. Gharehbaghi, F. Shemirani and M.D. Farahani, *J. Hazard. Mater.*, 2009, **165**, 1049.
21 M. Rozga, M. Koniecki, M. Dadlez and W. Bal, *Chem. Res. Toxicol.*, 2010, **23**, 336.
22 J. N. Hao and B. Yan, *J. Mater. Chem. A*, 2014, **2**, 18018.
23 G. Xie, Y. Shi, F. Hou, H. Liu, L. Huang, P. Xi, F. Chen and Z. Zeng, *Eur. J. Inorg. Chem.* 2012, 327.
24 D. M. Templeton and Y. Liu, *Chem. Biol. Interact.*, 2010, **188**, 267.
25 P. Wu, Y. Liu, Y. Liu, J. Wang, Y. Li, W. Liu and J. Wang, *Inorg. Chem.*, 2015, **54**, 11046.
26 T. W. Duan, B. Yan and H. Weng, *MICROPOR. MESOPOR. MAT.* 2015, **217**, 196.
27 S. Dang, E. Ma, Z. M. Sun and H. Zhang, *J. Mater. Chem.*, 2012, **22**, 16920.
28 F. Y. Yi, D. Chen, M. K. Wu, L. Han and H. L. Jiang, *ChemPlusChem*, 2016, **81**, 675.
29 J. Jia, J. N. Xu, S. Y. Wang, P. C. Wang, L. J. Gao, J. Chai, L. L. Shen, X. B. Chen, Y. Fan and L. Wang, *CrystEngComm*, 2016, **18**, 7126.

30 H. M. Hamid, *J. Braz. Chem. Soc.*, 2011, **22**, 1056.
31 L Li, Q Chen, Z Niu, X Zhou, T Yang and W Huang, *J. Mater. Chem. C.*, 2016, **4**, 1900.
32 L. Li, C. X. Li, Y. L. Ren, M. Song, Y. Ma and R. D. Huang, *CrystEngComm*, 2016, **18**, 7787.
33 I. T. Choi, M. J. Ju, S. H. Kang, M. S. Kang, B. S. You, J. Y. Hong, Y. K. Eom, S. H. Song and H. K. Kim, *J. Mater. Chem. A.*, 2013, **1**, 9114.
34 A. D. Finke, D. E. Gross, A. Han, Moore and J. S. Moore, *J. Am. Chem. Soc.*, 2011, **133**, 14063.
35 K. R. J. Thomas, J. T. Lin, Y.T. Tao and C.W. Ko, *J. Am. Chem. Soc.,* 2001, **123**, 9404.
36 N. Xie, J. Wang, Z. Guo, G. Chen and Q. Li. *Macromol, Chem. Phys.*, 2013, **214**, 1710.
37 H. J. Cheng, H. X. Tang, Y. L. Shen, N. N. Xia, W. Y. Yin, W. Zhu, X. Y. Tang, Y. S. Ma and R. X. Yuan, *J. Solid. State. Chem.*, 2015, **232**, 200.
38 M. Eddaoudi, Ł. Weseliński and R. Luebke, *Synthesis,* 2014, **46**, 596.
39 X. Liu, Y. Sun, Y. Zhang, F. Miao, G. Wang, H. Zhao, X. Yu, H. Liu and W. Y. Wong, *Org. Biomol. Chem.*, 2011, **9**, 3615.
40 B. Hu, X. Lv, J. Sun, G. Bian, M. Ouyang, Z. Fu, P. Wang and C. Zhang, *Org. Electron.,* 2013, **14**, 1521.
41 L. Li, S. Tang, X. Lv, M. Jiang, C. Wang and X. Zhao, *New J. Chem.*, 2013, **37**, 3662.
42 A. B. Kumar, J. M. Anderson and R. Manetsch, *Org. Biomol. Chem.*, 2011, **9**, 6284.
43 P. P. Bag, D. Wang, Z. Chen and R. Cao, *Chem. Commun.*, 2016, **52**, 3669.
44 H. J. Cheng, X. Y. Tang, R. X. Yuan and J. P. Lang, *CrystEngComm*, 2016, **18**, 4851.
45 J. Jia, X. Lin, C. Wilson, A. J. Blake, N. R. Champness, P. Hubberstey, G. Walker, E. J. Cussen and M. Schroder, *Chem. Commun.*, 2007, 840.
46 Y. Ooyama, N. Yamaguchi, I. Imae, K. Komaguchi, J. Ohshita and Y. Harima, *Chem. Commun.*, 2013, **49**, 2548.
47 J. R. Li, A. A. Yakovenko, W. Lu, D. J. Timmons, W. Zhuang, D. Yuan and H. C. Zhou, *J. Am. Chem. Soc.,* 2010, **132**, 17599.
48 G. M. Shedrick, SHELXL-97, program for Refining Crystal Structure Refinement, University of Göttingen, Germany, 1997.
49 A. L. Spek, PLATON, Amultipurpose crystallographic tool; Utrecht University: Utrecht, The Netherlands, 2001.
50 Y. Wang, C. Tan, Z. Sun, Z. Xue, Q. Zhu, C. Shen, Y. Wen, S. Hu, Y. Wang, T. Sheng and X. Wu, *Chem. Eur. J.,* 2014, **20**, 1341.
51 X. T. Zhang, L. M. Fan, W. L. Fan, B. Li, G. Z. Liu, X. Z. Liu and X. Zhao, *CrystEngComm*, 2016, **18**, 6914.
52 X. Y. Wan, F. L. Jiang, L. Chen, J. Pan, K. Zhou, K. Z. Su, J.D. Pang, G. X. Lyu and M. C. Hong, *CrystEngComm*, 2015, **17**, 3829.
53 S. Yuan, Y. K. Deng, W. M. Xuan, X. P. Wang, S. N. Wang, J. M. Dou and D. Sun, *CrystEngComm*, 2014, **16**, 3829.
54 Y. Gai, F. Jiang, L. Chen, M. Wu, K. Su, J. Pan, X. Wan and M. Hong, *Cryst. Growth Des.*, 2014, **14**, 1010.
55 L. Zhang, Y. Zhang, R. Wang, Z. Kang, X. Liu, D. Sun and Q. Meng, *CrystEngComm*,2015, **17**, 6591.
56 T. Liu, S. Wang and J. Bai, *CrystEngComm*, 2013, **15**, 5476.
57 X. Liu, Z. Xiao, A. Huang, W. Wang, L. Zhang, R. Wang and D. Sun, *New J. Chem.*, 2016, **40**, 5957.
58 J. M. Hao, B. Y. Yu, K. Van Hecke and G. H. Cui, *CrystEngComm*, 2015, **17**, 2279.
59 Yong-Liang Shao, Yan-Hui Cui, Jin-Zhong Gu, Alexander M. Kirillov, Jiang Wu and Y. W. Wang, *RSC Adv.*, 2015, **5**, 87484.
60 M. D. Zhang, L. Qin, H. T. Yang, Y. Z. Li, Z. J. Guo and H. G. Zheng, *Cryst. Growth Des.*, 2013, **13**, 1961.
61 H. Y. Liu, H. Wu, J. F. Ma, Y. Y. Liu, B. Liu and J. Yang, *Cryst. Growth Des.*, 2010, **10**, 4795.
62 Z. Su, J. Fan, T. A. Okamura, M. S. Chen, S. S. Chen, W. Y. Sun and N. Ueyama, *Cryst. Growth Des.*, 2010, **10**, 1911.
63 X. L. Wang, Y. F. Bi, G. C. Liu, H. Y. Lin, T. L. Hu and X. H. Bu, *CrystEngComm*, 2008, **10**, 349.
64 P. Deria, D. A. Gomez-Gualdron, W. Bury, H. T. Schaef, T. C. Wang, P. K. Thallapally, A. A. Sarjeant, R. Q. Snurr, J. T. Hupp and O. K. Farha, *J. Am. Chem. Soc.*, 2015, **137**, 13183.
65 U. Sheridan, J. F. Gallagher, A. Philippidis and J. McGinley, *Inorg. Chim. Acta*, 2015, **421**, 50.
66 P. Deria, D. A. Gomez-Gualdron, I. Hod, R. Q. Snurr, J. T. Hupp and O. K. Farha, *J. Am. Chem. Soc.*, 2016, **138**, 14449.
67 P. Deria, J. Yu, R. P. Balaraman, J. Mashni and S. N. White, *Chem. Commun.*, 2016, **52**, 13031.
68 H. Zhang, C. Lin, T. Sheng, S. Hu, C. Zhuo, R. Fu, Y. Wen, H. Li, S. Su and X. Wu, *Chem. Eur. J.,* 2016, **22**, 4460.
69 S. Wang, L. Shan, Y. Fan, J. Jia, J. Xu and L. Wang, *J. Solid. State. Chem.*, 2017, **245**, 132.
70 A. C. Harris and I. L. Weatherall, *Journal of the Royal Society of N. Z.*, 1990, **20**, 253.
71 T. Smith and J. Guild, *Trans. Opt. Soc.*, 1932, **33**, 73.
72 M. Lalonde, W. Bury, O. Karagiaridi, Z. Brown, J. T. Hupp and O. K. Farha, *J. Mater. Chem. A*, 2013, **1**, 5453.
73 Y.J. Hu, J. Yang, Y. Y. Liu, S. Song and J. F. Ma, *Cryst. Growth Des.* 2015, **15**, 3822.
74 L. L. Lv, J. Yang, H. M. Zhang, Y. Y. Liu and J. F. Ma, *Inorg. Chem.* 2015, **54**, 1744.
75 J. Li, L. Li, H. Hou and Y. Fan, *Cryst. Growth Des.*, 2009, **9**, 4504.
76 F. Li, J. J. Hu, L. L. Koh and T. S. Hor, *Dalton Trans.*, 2010, **39**, 5231.
77 K. Suman, F. Baig, R. kant, V. K. Gupta, S. Mandal and M. Sarkar, *RSC Adv.*, 2014, 4, 36451.
78 A. Pal, S. Chand, S. Senthilkumar, S. Neogi and M. C. Das, *CrystEngComm*, 2016, **18**, 4323.
79 L. Granato, S. Laurent, L. Vander Elst, K. Djanashvili, J. A. Peters and R. N. Muller, *Contrast Media Mol. Imaging,* 2011, **6**, 482.
80 G. M. Pawar, J. B. Sheridan and F. Jäkle, *Eur. J. Inorg. Chem.* 2016, 2227.
81 M. Taddei, A. Ienco, F. Costantino and A. Guerri, *RSC Adv.*, 2013, **3**, 26177.
82 K. Akhbari, K. Alizadeh, A. Morsali and M. Zeller, Inorg. Chim. Acta, 2009, **362**, 2589.
83 Y. Han, H. Xu, Y. Liu, H. Li, H. Hou, Y. Fan and S. R. Batten, *Chem. Eur. J.*, 2012, **18**, 13954.
84 Z. Lei, X. L. Pei, Z. G. Jiang and Q. M. Wang, *Angew. Chem. Int. Ed.*, 2014, **53**, 12771.
85 Z. Z. Lu, R. Zhang, Z. R. Pan, Y. Z. Li, Z. J. Guo and H. G. Zheng, *Chem. Eur. J.*, 2012, **18**, 2812.

View Article Online
DOI: 10.1039/C7CE00361G

Graphical Abstract

Five coordination polymers, based on a novel carbazole-based ligand, show a linear correlation to Ni^{2+} and Eu^{3+} concentration.